Structural Changes during Polystyrene Orientation: A Study of Optical Birefringence and Wide Angle X-Ray Scattering

G. VANCSO,[1,*] D. SNÉTIVY,[2] and I. TOMKA[2]

[1] University of Toronto, Department of Chemistry, Toronto, Ontario M5S 1A1, Canada, and [2] Swiss Federal Institute of Technology, Institute for Polymers, ETH-Zentrum, CH-8092 Zürich, Switzerland

SYNOPSIS

Results of coupled optical birefringence and wide-angle X-ray scattering (WAXS) measurements on uniaxially oriented, atactic, glassy polystyrene (PS) samples are reported. Orientations were achieved in tensile test experiments performed slightly above the glass transition temperature. The elongated samples were quenched after orientation. The applied force was kept constant during cooling. The second order moments of the chain orientation distribution function (ODF) were calculated from the azimuthal profile of the scattered X-ray intensity from measurements made on five PS samples with different degrees of orientation. For ODF calculations the first, equatorial halo was used. The influence of the second, meridional halo was removed by resolving the WAXS patterns into three peaks. The intrinsic azimuthal linewidth of the WAXS profile was estimated and taken into account in the ODF calculations. The magnitude of the intrinsic birefringence Δn_{int} was determined using the linear relationship between the birefringence and the second order moment of the ODF. A value for Δn_{int} of -0.05 was obtained. This result was used to calculate the angle between the normal plane of the benzene ring and the chain axis. A comparison with previously published results indicates that the average relative orientation of the benzene ring with respect to the chain axis was changing in our samples during stretching. This structural difference is attributed to strong deformation of the network and retarded relaxation during sample preparation.

INTRODUCTION

Anisotropy in polymeric glasses due to chain orientation is a phenomenon of great technical and theoretical importance (for a review, see Ref. 1). Orientation may or may not be desired, depending on the final use of the material. Incident orientation, e.g., in injection molding, is usually regarded as disadvantageous, while the textile and the packaging industries make extensive use of uni- and biaxially oriented plastics. High performance composite materials are also often reinforced by oriented synthetic fibers. Studies of orientation play therefore a central role for both product characterization and a better understanding of structure–property relations.[1]

In this paper only the anisotropy of an amorphous, glassy polymer with fiber symmetry will be considered. In such cases, the simplest way to characterize the orientation of the backbone chain is to determine the second-order moment of the chain orientation distribution function (ODF), the so-called Hermans orientation factor f [1]:

$$f = (1/2)(3\langle\cos^2\vartheta\rangle - 1) \qquad (1)$$

where ϑ is the angle between the fiber axis and chain segments and $\langle\cos^2\vartheta\rangle$ represents the average of $\cos^2\vartheta$ values taken over their spatial distribution. Although the value of f does not give a complete characterization of the orientation, it can describe the anisotropy of many physical properties like infrared absorption, refractive index, etc. For perfect orientation $\vartheta = 0°$, i.e., $f = 1$, the macromolecular chains are perfectly aligned and the corresponding maximum in the birefringence Δn is defined as the

* To whom correspondence should be addressed.

Journal of Applied Polymer Science, Vol. 42, 1351–1359 (1991)
 CCC 0021-8995/91/051351-09$04.00

intrinsic value, Δn_{int}.[1] If the value of Δn_{int} is known, a simple optical measurement will yield the Hermans orientation factor by applying the following formula:

$$f = \Delta n / \Delta n_{int} \quad (2)$$

The magnitude of Δn_{int} for a given polymer can be determined from a series of samples of defined orientation by performing measurements of Δn and f. The values of f may be determined by measuring the dichroitic ratio,[1-4] the wide-angle X-ray scattering (WAXS) pattern,[1,5-13] or by using other methods which are sensitive to chain orientation. However, it must be pointed out that the possibility of having different orientation behavior for the main chain as compared to side groups with some rotational degree of freedom has always to be borne in mind. For example, in PS the benzene ring can rotate about the chemical bond which connects it with the main chain. For a rigorous description of the anisotropy, its position relative to the chain must be specified in addition to the chain orientation.

EXPERIMENTAL

Samples

Atactic polystyrene was supplied by BASF Ag. Our test specimens were prepared from granulates type PS 158 K. DSC measurements yielded a glass transition temperature range between 97 and 114°C with an inflection point at 108°C. GPC measurements combined with a low angle laser light scattering detector (Chromatix KMX-6) yielded a weight average molar mass of $M_w = 2.87 \times 10^5$ and a polydispersity of $M_w/M_n = 2.4$.[14]

Polystyrene granulate was dried *in vacuo* for 2 h at 70°C and then pressed into plates of 2 and 4 mm thicknesses by a compression molding press operating at 250°C for 30 min. Thermal degradation during sample preparation could be excluded since a comparison of the weight average molar mass and the optical absorption of the starting and pressed polymers showed no differences.[14] Tensile test specimen were cut from the molded plates and drawn on a tensile test machine at temperatures between 108 and 112°C (±0.5°C) at different clamp speeds. The elongation was stopped at certain strains, the force was kept constant, and the samples were quenched (by applying a cooled air stream) within ca. 20 s below the glass transition range. Tensile test diagrams of the measured PS samples are shown in Figure 1. Temperature and geometry inhomogenities during stretching and quenching resulted in a maximal (λ_{max}) and minimal elongation value.

Parameters of the orientation and some characteristics of the samples are summarized in Table I.

X-ray measurements were performed on 20 × 8 mm broad samples with different thicknesses (see Table I). The samples were cut from the central part of the stretched, frozen tensile test specimens with the highest orientation. The orientation in all the samples used were homogeneous over a multiple of the length scale of the scattering volume within ±2% for the lowest and ±0.3% for the highest orientation. The diameter of the X-ray beam at the sample surface was 0.6 mm. This is significantly smaller than the characteristic size of the central

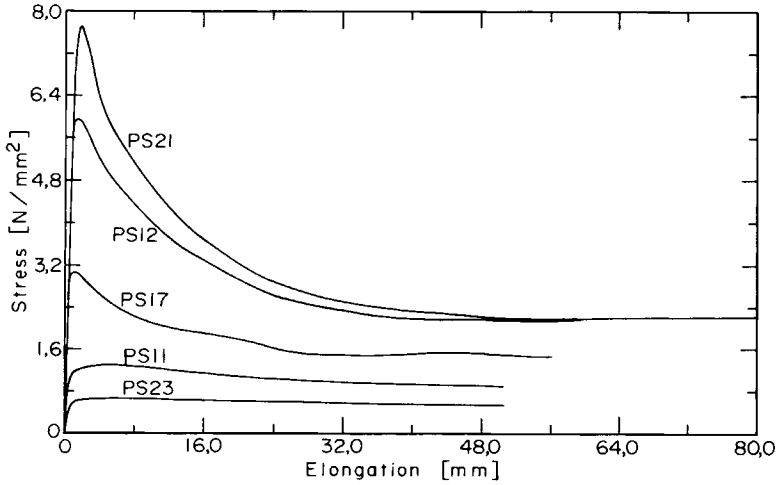

Figure 1 Tensile test diagrams (force vs. clamp movement) for the five PS samples investigated.

Table I Parameters of the Orientation Process and Some Sample Characteristics

Sample No.	Tensile Test Characteristics: Temperature (°C)	Tensile Test Characteristics: Clamp Speed (mm/min)	Sample Characteristics[a]: Thickness[b] (mm)	Sample Characteristics[a]: λ_{max}[c]
PS23	112.0	10	1.22	2.8
PS11	112.0	50	1.26	2.6
PS17	108.5	50	1.07	4.0
PS12	108.3	100	0.96	4.0
PS21	108.0	100	1.55	6.0

[a] For the quenched samples.
[b] The starting sample thickness was 2 mm except for the sample PS21 which was 4 mm.
[c] Approximate value from the change of the sample geometry determined by the change of a pattern brought on the sample surface prior to orientation.

sample area (ca. 3 mm), where the optical retardation varies less than $\lambda/4$.

MEASUREMENTS AND EVALUATION

Birefringence Measurements

For birefringence measurements a classical stress-optical device was applied.[15] Anisotropic PS samples were put between crossed polarizers which were illuminated by monochromatic light with wavelength $\lambda = 546$ nm. Photographs were taken of the resultant optical pattern through the analyzer. The black–white interference pattern arises from the optical retardation changes due to the frozen anisotropy. Between two black maxima the difference in the optical retardation, Γ, is equal to the applied wavelength. By simply counting the maxima from the sample edge in the stretching direction, the magnitude of Γ can be determined with an accuracy of approximately $\pm\lambda/4$. The corresponding birefringence Δn can then be calculated with the sample thickness d:

$$\Delta n = \Gamma/d \tag{3}$$

Typical photographs of the optical retardation pattern taken from the samples PS21 and PS12 are shown in Figure 2. For sample PS12 the number of transitions from the sample edge to the center was 38; the same for PS21 was 82.

Wide Angle X-Ray Scattering (WAXS) Measurements

WAXS measurements were performed by a Siemens D 500 diffractometer equipped with a Huber texture goniometer. The Eulerian cradle of the texture goniometer allowed rotation of the specimen while maintaining the diffraction angle constant along the sample coordinate axes. No corrections were made for absorption, polarization, multiple diffraction, or incoherent scattering. Air scattering was taken into account by subtracting background intensity. The continuous background was estimated by calculating the equation of the convex linear-by-parts envelope of the diffractogram.[16] A typical WAXS spectrum of Polystyrene (sample PS11) after background subtraction is shown in Figure 3. The measured intensities are plotted at every $2\theta = n$, $n = 2, \ldots, 500$. The WAXS pattern for $2° \leq 2\theta \leq 50°$ is obviously a sum of at least three overlapping halos. In order to deduce information about the individual components, a numerical decomposition of the spectrum was performed. We resolved the WAXS patterns of Polystyrene into three components describing the spectrum envelope $I(x)$ $(x = 2\theta)$ by the formula:

$$\begin{aligned} I(x) = {} & A_1 \exp\{-[(x - x_1)/\sigma_1]^2\} \\ & + A_2/\{1 + [(x - x_2)/\sigma_2]^2\} \\ & + A_3/\{1 + [(x - x_3)/\sigma_3]^2\} \end{aligned} \tag{4}$$

i.e., by a sum of one Gaussian and two Lorentzian functions, where the unknown parameters A_1, A_2, and A_3 are the amplitudes; x_1, x_2, and x_3 are the line centers; and σ_1, σ_2, and σ_3 are the half-linewidths, respectively. To obtain the values of the unknown parameters, Marquardt–Levenberg nonlinear regression analyses (NLRA)[17] were performed for every individual WAXS pattern measured at different azimuth angles over the interval $2° \leq 2\theta < 60°$ for $2\theta = 2.0 + n \cdot 0.5$, $n = 0, 1, 2, \ldots, 116$. NLRA fits were performed by using the IMSL Double Precision FORTRAN program library[18] on an IBM PC-AT. We choose eq. (4) to fit the spectral envelope while this combination of Gaussians and Lorentzians gave the smallest sum of squared residuals. Figure 3 displays the fitted envelope and the components together with the experimental data for the sample PS11. The fit is excellent except for a systematic deviation for $2\theta < 6°$. This is a result of automatic background subtraction which overcorrects the measured WAXS intensities in the small angle scattering regime.

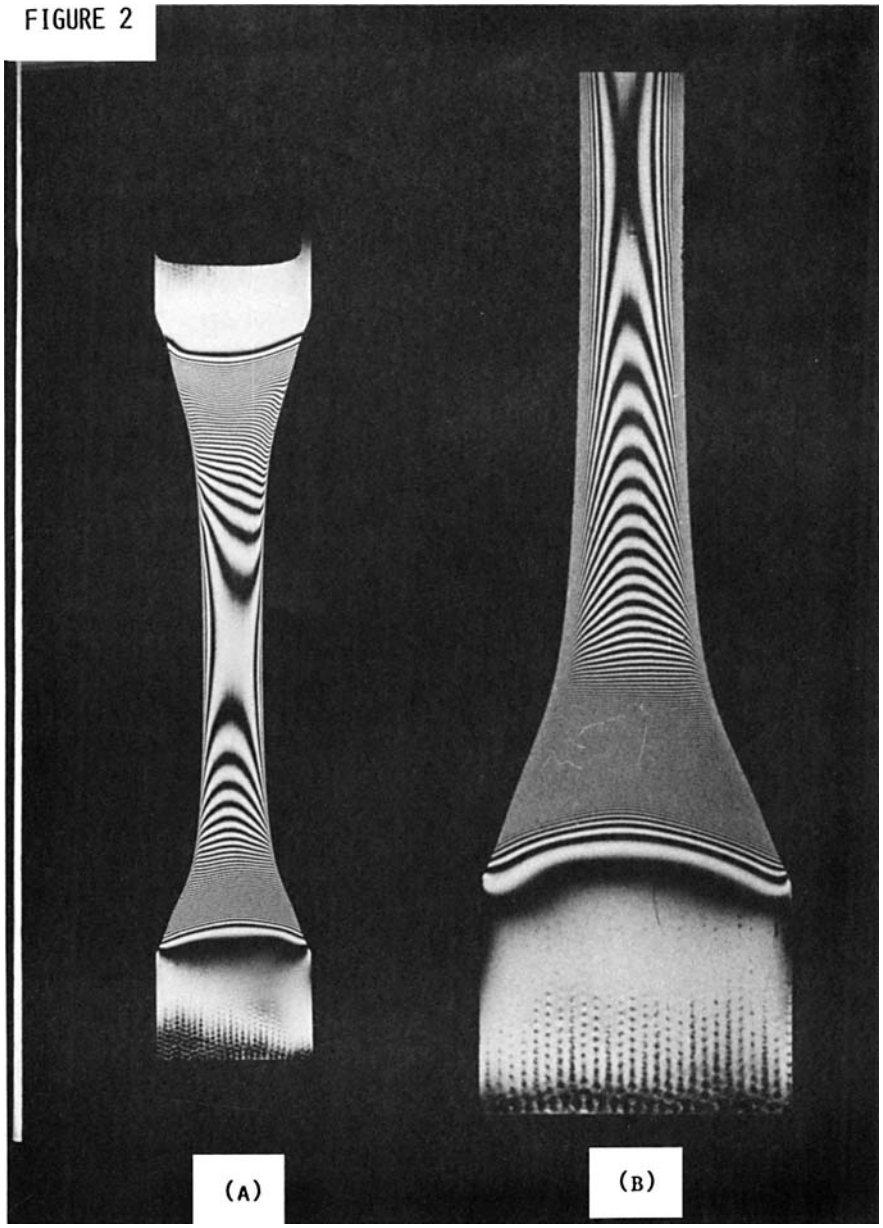

Figure 2 Fringe pattern (optical retardation) for two PS samples with different degrees of orientation: (a) PS12; (b) PS21.

For anisotropic samples the azimuthal X-ray scattering intensity $I(\chi)$ (the azimuthal profile) contains information about the ODF. The ODF and its moments can be calculated from $I(\chi)$ by using several procedures.[8,9,11,13] However, for all methods the structural origin of the halos and the type of texture has to be known.

In this paper we apply the technique of Lovell and Mitchell,[13] which makes use of a series expansion of even-order Legendre polynomials (P_{2n})[19] of the full azimuthal intensity profile.[13] This technique can be applied to any reflection with known azimuthal angle if both the ODF and the molecular (segmental) scattering have cylindrical symmetry. As a special case, for an equatorial reflection the orientation factor is written as

$$f = \langle P_2(\cos\vartheta)\rangle = (-2)\int_0^{\pi/2} I(\chi)P_2(\cos\chi)\sin\chi\, d\chi \Big/ \int_0^{\pi/2} I(\chi)\sin\chi\, d\chi \qquad (5)$$

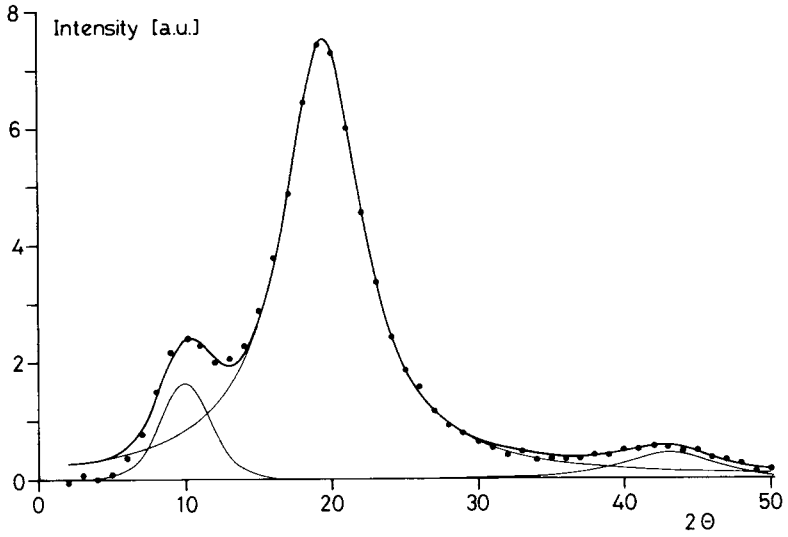

Figure 3 WAXS pattern of the sample PS11 at $\chi = 90°$ and the decomposition of the diffractogram into three components: (○) measured and corrected data; (——) fitted envelope; (——) fitted individual components.

where χ is measured from the fiber axis, $I(\chi)$ is the azimuthal reflexion profile at constant θ, and P_2 (cos χ) is the second-order Legendre polynomial.[19] Equation (5) holds strictly speaking for sharp, crystalline reflexes. In polymeric glasses, however, the haloes are diffuse. Even a perfectly aligned polymeric glass would give diffuse spots with characteristic dimensions corresponding to the degree of order of the reflecting structural units. This unknown intrinsic azimuthal width δ_{int} results in smaller calculated orientation factors then the true values.[20] Pick et al. calculated the effect of δ on the first even order moments of the ODF. For a typical value $\delta_{int} = 20°$, ratios for the observed/true values of the orientation factors are for $\langle P_2 \rangle$ to approx. 0.7, for $\langle P_4 \rangle$ to approx. 0.4 and for $\langle P_6 \rangle$ to approx. 0.2. We estimated half-width δ of the azimuthal profile using the following equation:

$$\delta = \left(\int_0^{\pi/2} [I(\chi) - I(0)]\, d\chi \right) \Big/ ([I(\pi/2) - I(0)]) \quad (6)$$

The values of δ were plotted as a function of the observed f and extrapolated to $f = 1$ (perfect alignment). The extrapolated value for δ at $f = 1$ was used to estimate the intrinsic width δ_{int}. A corresponding correction factor K for f was estimated by using results of Pick et al.[20] All orientation factors discussed in this study were corrected according to the following equation:

$$f = K \cdot f_{obs} \quad (7)$$

where the values for f_{obs} were determined from eq. (5).

RESULTS AND DISCUSSION

Birefringence and WAXS measurements were performed on five oriented PS samples. The WAXS pattern for the sample PS21 for scattering angles 2θ between 2° and 60° and for azimuth angles 0° (equator) and 90° (meridian), supposing vertical fiber axis, is shown in Figure 4. The first halo at $2\theta = 9.9°$ has an equatorial character (see also Ref. 21). The second, meridional halo is located around $2\theta = 18.5$–$19.5°$ while its position is shifted towards smaller scattering angles approaching the equator from the meridian. The intensity of the third, meridional halo at $2\theta = 41°$ is weak. According to earlier assignments,[11] the meridional maximum corresponds to correlations between phenyl groups which may not belong to the same molecule. A shift in the position means a change in the spacing between diffracting units with sample rotation. It was concluded by Windle[22] that the equatorial maximum corresponds to correlations between loosely packed phenyl stacks which are organized between the chains. These stacks will be oriented parallel to the PS chains, i.e., the corresponding X-ray scattering is equatorial. We note that the exact assignation of

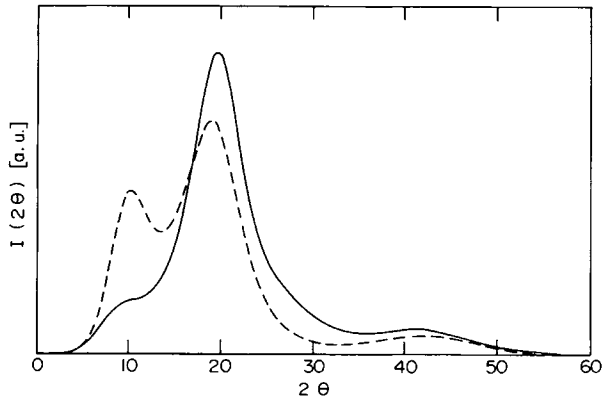

Figure 4 X-ray scattering intensity for amorphous, uniaxially drawn PS (sample PS21): (· · ·) intensity along the equator ($\chi = 90°$); (——) intensity along the meridian ($\chi = 0°$).

the halos is the subject of controversy.[22,23] It has been dealt with in several papers[11,20,22-24] and is the subject of a forthcoming analysis.[25]

Figure 5 shows the azimuthal intensity profile for the five PS samples measured at $2\theta = 9.9°$ between $\chi = 0$ and 90°. Because of the already mentioned contribution of the meridional halo, the azimuthal profiles shown in Figure 5 cannot be used to calculate the orientation factors. Therefore, complete WAXS patterns were measured for the five investigated PS samples at 0°, 22.5°, 33.75°, 45°, 56.25°, 67.5°, 78.75°, and 90° azimuth angles over the scattering range $2° < 2\theta < 60°$. Each WAXS pattern was decomposed by using eq. (4) and the previously described NLRA procedure. The obtained true amplitudes of the first halo do not contain contributions from the second halo and can be used for further analysis. The azimuthal profile for each sample was approximated by using the amplitudes from eight azimuthal angles and fitting the following function:

$$I(\chi) = a \sin^{2b}(\chi) + I(0°) \qquad (8)$$

where $I(0°)$ denotes the intensity at the meridian. This simple function was chosen for two reasons: (1) It gave a very good fit to the profile; and (2) its derivative at $\chi = 0°$ and $\chi = 90°$ is zero as must be the case for equatorial intensities. The fitted $I(\chi)$ was then substituted into eq. (5) and the integration was performed numerically by using the Romberg extrapolation.[18] The intrinsic azimuthal linewidth was then calculated from the fitted line shapes substituting $I(\chi)$ from eq. (8) into eq. (6). The values for δ as a function of the corrected orientation factor f are plotted in Figure 6. The extrapolation to $f = 1$ yielded an estimate for δ_{int} of 23°. With this intrinsic width, the value of the correction factor K in eq. (7) becomes 1.47. We applied this K factor to calculate the corrected ("true") orientation factor f_{corr} from the f_{obs} determined using eq. (5). The values of f_{corr} are plotted against the birefringence in Figure 7. The relationship is linear with a regression coefficient $r = 0.998$ and has the following numerical form:

$$f_{true} = -20.64\ \Delta n + 0.0036 \qquad (9)$$

An extrapolation to $f = 1$ corresponds to perfectly aligned chains and results in the following value for the intrinsic birefringence Δn_{int}:

$$\Delta n_{int} = -0.048$$

We note that a similar calculation, made without taking into account the correction for the intrinsic width, results in a value of $\Delta n_{int} \approx -0.07$.

All values for Δn_{int} of atactic PS reported previously were determined using combined optical and infrared dichroitic measurements. Additionally, the orientation of those samples was significantly lower than ours ($f < 0.2$ typically). Some results available together with the corresponding citations are summarized in Table II. In Ref. 4 the orientation factor

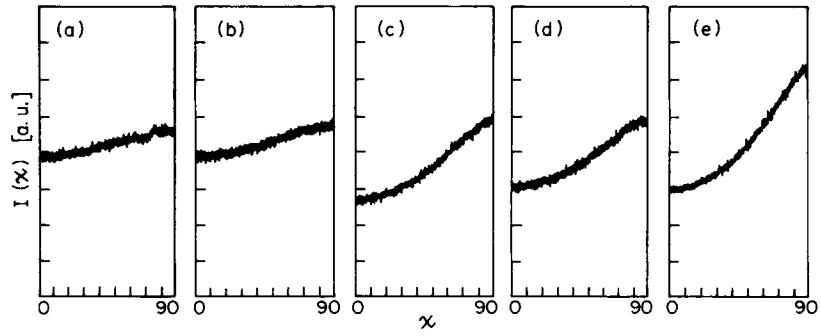

Figure 5 Azimuthal WAXS intensity profiles of the five investigated PS samples measured at $2\theta = 9.9°$: (a) PS23; (b) PS11; (c) PS17; (d) PS12; (e) PS21.

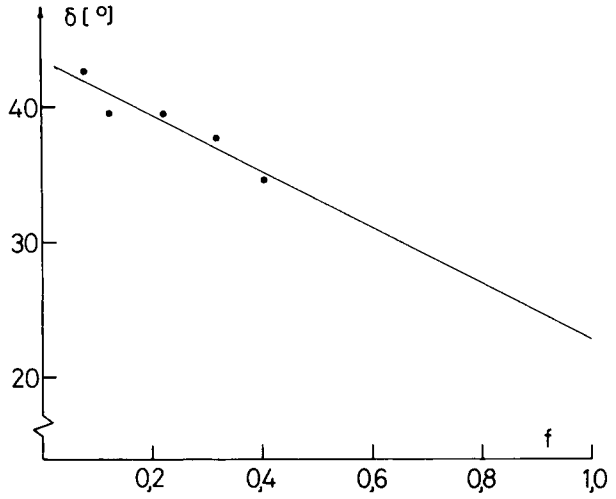

Figure 6 The azimuthal half width of the WAXS pattern at $2\theta = 9.9°$ as a function of the observed orientation factor.

was calculated from the $-CH_2-$ symmetrical stretching at 2850 cm^{-1}, assuming that the corresponding transition dipole moment makes an angle β of 90° with the chain axis. Later studies[26] validated a value of 70° for β. To obtain a corrected value, we performed a multiplication by 1.54. This factor was obtained using the relationship between the orientation factor and the dichroitic ratio R[26]:

$$f = [(R - 1)/(R + 2)] \times [(R_0 + 2)/(R_0 - 1)] \quad (10)$$

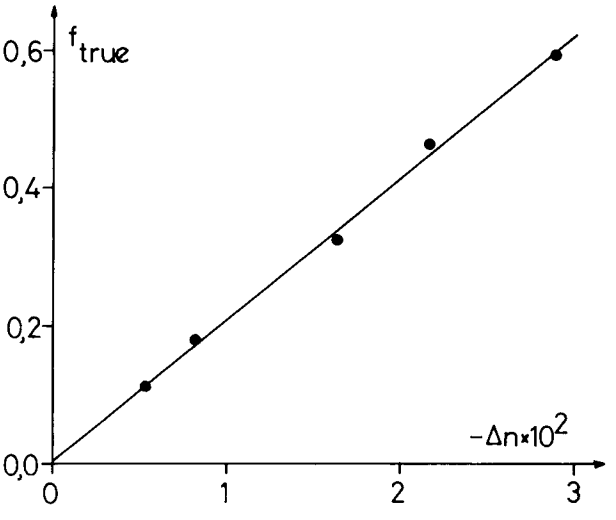

Figure 7 The birefringence Δn as a function of the corrected orientation factor f_{true} for the five investigated PS samples.

where $R_0 = 2 \cdot \cot^2(\beta)$. Performing the above correction, we obtained $\Delta n_{int} = -0.10$ with the data from Ref. 4 which is in agreement with all the other data in Table II.

It is obvious that our result for Δn_{int} is significantly smaller than the data summarized in Table II. The first question one would ask is: In what ways do our samples differ from the others? We have mentioned already that our samples were much more strongly oriented than those in any cited work. We stretched our samples just slightly above the glass transition temperature at high clamp speeds. In addition, we kept the tensile force constant during the quenching of the oriented samples, thus preventing the relaxation of the orientation to a large extent during cooling. We believe that during our "brutal" procedure, used to achieve the highest possible orientations, the average angle closed by the normal of the phenyl rings and the chain axis changed. Due to the rotation of the phenyl group about the chemical bond connecting it with the main chain, the difference in the segment polarizability both perpendicular and parallel to the chain axis, and hence the intrinsic birefringence, were also changed. The phenyl ring position with respect to the chain can be quantitatively characterized using calculated results for the intrinsic birefringence as a function of the benzene ring orientation. The value of the birefringence of atactic PS was calculated by several authors[27] from the bond polarizabilities and valence angles and the following expression was obtained:

$$\Delta n_{int} = 0.194 - 0.51\langle \cos^2\omega \rangle \quad (11)$$

where ω is the angle closed by the normal of the plane of the benzene ring and the chain axis. According to a very careful analysis of the IR-dichroism[28] the average magnitude of ω prior to orientation is $\omega_1 \approx 38°$ (with ca. ±4° uncertainty). Using eq. (11), this value results in $\Delta n_{int} \approx -0.156$. With $\Delta n_{int} = -0.048$ from this study, one obtains $\omega_2 \approx 46°$ for the inclination of the benzene ring in the fully ori-

Table II Intrinsic Birefringence of Atactic Polystyrene Determined by Coupled Optical and IR-Dichroitic Measurements

Source	2	3	4
$-\Delta n_{int}$	0.10 (±0.05)	0.10	0.16 0.10[a]

[a] For explanation, see text.

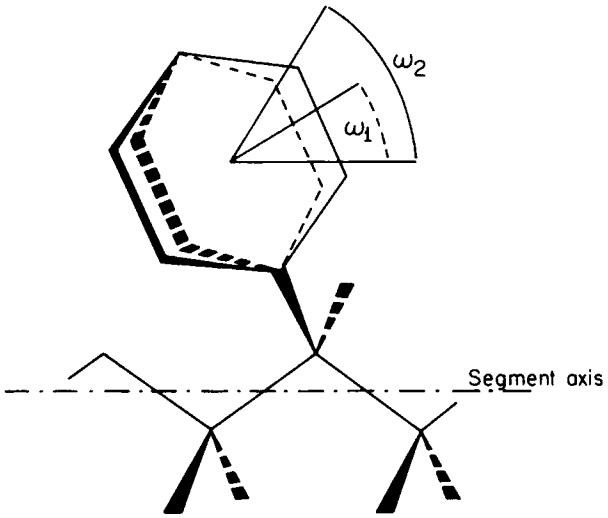

Figure 8 The average orientation of a phenyl substituent in a PS segment prior to sample elongation [$\omega_1 \approx 36°$ ($\cdots$)] and for the fully stretched configuration [$f = 1$; $\omega_2 \approx 46°$ (——)] as suggested in the text.

ented configuration. The monomer segment in these two limiting cases is illustrated in Figure 8.

According to the generalization of the relationship between mechanical stress (σ) and birefringence (Δn) in a temporary network (polymer melt), the stress-optical coefficient (SOC) $\Delta n/\sigma$ is expected to be constant during isothermal uniaxial deformation.[29] Results of elongation experiments on PS melts have been reported in the literature showing deviations in SOC from linearity at high stresses.[30] In this nonlinear regime, stress increased more rapidly with birefringence, in agreement with very recent data[31] showing a clear and systematic deviation of SOC from the expected linearity. These results can also be explained by supposing a change in the phenyl ring position during elongation. These facts argue for a careful analysis of continuum assumptions made in polymer rheology.

Finally we note that both IR dichroitic and WAXS measurements to characterize chain orientation involve complications. The WAXS azimuthal profiles used for the determination of the orientation factors have to be corrected very carefully with respect to overlaps in the neighboring haloes and to the intrinsic azimuthal width. The difficulty of an IR dichroitic analysis is that one should know the angle of the transition dipole moment vector closed by the chain axis for the studied IR vibration. Moreover, IR dichroism is usually only applicable to thin films. (This prevented us from checking our values of f_{true}.) Once the intrinsic azimuthal linewidth is known, a WAXS analysis results also in higher order moments of the orientation distribution function and therefore is the method of choice in characterizing chain orientation.

The authors acknowledge financial support by the Swiss National Scientific Foundation (Grant No. 2.046-0.86), by the Swiss Federal Institute of Technology (ETH, Zürich) and by the Ontario Center for Materials Research. They express their gratitude to BASF Ag., Ludwigshafen (BRD) for the donation of PS granulate, to Mr. Victor Foyle for his valuable comments concerning the manuscript, to Mr. H. U. Hoppler for the supplement of his data concerning the characteristics of the starting samples, and to Dr. T. Q. Nguyen, EPFL, Lausanne (Switzerland) for his help in the tensile test experiments.

REFERENCES

1. I. M. Ward, Ed., *Structure and Properties of Oriented Polymers*, Applied Science, London, 1975.
2. D. Lefebre, B. Jasse, and L. Monnerie, *Polymer*, **23**, 706 (1982).
3. R. Neuert, H. Springer, and G. Hinrichsen, *Coll. Polym. Sci.*, **263**, 392 (1985).
4. M. F. Milagin, A. D. Gabarayeva, and I. I. Shiskhin, *Polym. Sci. USSR*, **A12**, 577 (1977).
5. O. Kraty, *Colloid Polym. Sci.*, **64**, 313 (1933).
6. L. E. Alexander, *X-Ray Diffraction Methods in Polymer Science*, Wiley-Interscience, New York, 1969.
7. A. H. Windle, in *Developments of Oritented Polymers—1*, I. M. Ward, Ed., Applied Science, London, 1982.
8. H. J. Biangardi, *J. Polym. Sci. Polym. Phys. Ed.*, **18**, 903 (1980).
9. H. J. Biangardi, *Makromol. Chem.*, **183**, 1785 (1982).
10. W. Kast, *Kolloid Z.*, **114**, 23 (1949).
11. M. May and C. Walther, *Plaste Kautschuk*, **22**, 418 (1975); M. May, *J. Polym. Sci. Polym. Symp.*, **58**, 23 (1977).
12. H. D. Deas, *Acta Cryst.*, **5**, 542 (1952).
13. R. Lowell and G. R. Mitchell, *Acta Cryst.*, **A37**, 135 (1981).
14. H. U. Hoppler, private communication.
15. G. Messmer, *Spannungsoptik*, Springer-Verlag, Berlin, 1939.
16. *Getting Started with the DACO-MP*, Instruction Manual, Siemens AG, Karlsruhe, 1984.
17. K. Levenberg, *Quart. Appl. Math.*, **2**, 164 (1944); D. W. Marquardt, *J. Soc. Ind. Appl. Math.*, **11**, 431 (1963).
18. IMSL Fortran Subprogram Library for IBM-Professional Fortran, Houston, TX, 1985.
19. G. A. Korn and T. M. Korn, *Mathematical Handbook for Scientists and Engineers*, McGraw-Hill, New York, 1968.

20. M. Pick, R. Lovell, and A. H. Windle, *Polymer,* **21,** 1017 (1980).
21. R. Lowell and A. H. Windle, *Polymer,* **17,** 488 (1976).
22. A. H. Windle, *Pure Appl. Chem.,* **57,** 1627 (1985).
23. H. R. Schubach, Diplomarbeit (Graduate Thesis), University of Ulm (BRG), 1984.
24. H. G. Kilian and K. Boueke, *J. Polym. Sci.,* **58,** 311 (1962).
25. A. Margraf and G. Vancso, to appear.
26. R. Zbinden, *Infrared Spectroscopy of High Polymers,* Academic, New York, 1964.
27. E. F. Gurnee, *J. Appl. Phys.,* **25,** 1232 (1954); R. S. Stein, *J. Appl. Phys.,* **32,** 1280 (1961).
28. B. Jasse and J. L. Koenig, *J. Polym. Sci. Polym. Phys. Ed.,* **17,** 799 (1979).
29. A. S. Lodge, *Kolloid Z.,* **171,** 46 (1960).
30. T. Matsumoto and D. C. Bogue, *J. Polym. Sci. Polym. Phys. Ed.,* **15,** 1663 (1977).
31. F. Dinkel, H. U. Hoppler, and T. Tomka, Spannugsoptische Untersuchungen an Polystyrol oberhalb der Glasübergangstemperatur, Preprint, to appear.

Received June 23, 1989
Accepted June 12, 1990